# AUTHOR QUERY FORM

| | | |
|---|---|---|
| ELSEVIER | **Book: Satellite Soil Moisture Retrieval**<br>**Chapter: 00018** | **Please e-mail your responses and any corrections to:**<br>**E-mail: P.Chandramohan@elsevier.com** |

Dear Author,

Any queries or remarks that have arisen during the processing of your manuscript are listed below and are highlighted by flags in the proof. (AU indicates author queries; ED indicates editor queries; and TS/TY indicates typesetter queries.) Please check your proof carefully and answer all AU queries. Mark all corrections and query answers at the appropriate place in the proof using on-screen annotation in the PDF file. For a written tutorial on how to annotate PDFs, click http://www.elsevier.com/__data/assets/pdf_file/0007/98953/Annotating-PDFs-Adobe-Reader-9-X-or-XI.pdf. A video tutorial is also available at http://www.screencast.com/t/9OIDFhihgE9a. Alternatively, you may compile them in a separate list and tick off below to indicate that you have answered the query. **Please return your input as instructed by the project manager.**

| **Location in Chapter** | **Query / remark?** | |
|---|---|---|
| AU:6, page 364 | Allen et al. (1998) has been changed to Allen (1998) to match the reference list. Please check. | ☐ |
| AU:7, page 364 | Drusch et al. (2007) has been changed to Drusch and Viterbo (2007) to match the reference list. Please check. | ☐ |
| AU:8, page 364 | Dirmayer et al. (2000) has been changed to Dirmayer (2000) to match the reference list. Please check. | ☐ |
| AU:9, page 367 | Please check the mixed usage of "$H_i$" and "$\mathbf{H}_i$." | ☐ |
| AU:10, page 370 | Fascetti et al. (2015) has been changed to Fascetti et al. (2016) to match the reference list. Please check. | ☐ |

| | |
|---|---|
| AU:11, page 371 | Reichle et al. (2004) has been changed to Reichle and Koster (2004) to match the reference list. Please check. |
| AU:12, page 378 | Please check the inserted author names. |

Section V

# Future Challenges in Soil Moisture Retrieval and Applications

Chapter 18

c0090

# Soil Moisture Retrievals Based on Active and Passive Microwave Data: State-of-the-Art and Operational Applications

J. Muñoz-Sabater*, A. Al Bitar† and L. Brocca‡

*European Centre for Medium Range Weather Forecasts, Reading, United Kingdom, †Centre d'Études Spatiales de la Biosphère, Toulouse, France, ‡Research Institute for Geo-Hydrological Protection, National Research Council, Perugia, Italy

s0010

## 1 INTRODUCTION

p0020 This chapter is organized in five main parts. In the first one, operational soil moisture retrievals based on active C-band data from the advance scatterometer (ASCAT) sensor on board the European meteorological operational program (MetOp) (Figa-Saldana et al., 2002) are considered, and the potential of these data for flood and landslide forecasting is demonstrated. The region of operational application is Italy. The production of soil moisture retrievals from ASCAT data (also in missions such as the Canadian RADARSAT-2 or the first of a series of European Sentinel missions, Sentinel-1) is based on the change detection algorithm. Details about this methodology can be consulted in Wagner et al. (1999, 2013) and Naeimi et al. (2009). This has been one of the first operational retrieval approaches of soil moisture from backscatter information. Recently a generalization of change detection to multiple regression using cumulative distribution function (CDF) transformations was applied to RADARSAT-2 data and validated over Berambadi watershed, South India (Tomer et al., 2015). This part of the chapter focuses on the use of the ASCAT soil moisture product for floods and landslides operational prediction from National and Regional Civil Protection Centres in Italy.

p0025 The second part focuses on soil moisture retrievals based on low frequencies passive microwave data. Soil moisture retrievals have been obtained from

Satellite Soil Moisture Retrieval. http://dx.doi.org/10.1016/B978-0-12-803388-3.00018-8

C-band passive microwaves using the advanced microwave scanning radiometer for earth observing system (AMSR-E) sensor data on NASA's aqua satellite (Njoku et al., 2003; Owe et al., 2008). However, L-band is more optimal for soil moisture estimation, because it is less sensitive to roughness and vegetation effects. At these frequencies, the atmosphere is nearly transparent; therefore, both C- and L-band sensors provide all-weather coverage (Eagleman and Lin, 1976; Wang and Choudhury, 1981; Jackson and Schmugge, 1991). L-band acquisition for global soil moisture retrievals has been available since a few weeks after the launch in Nov. 2009 of the Soil Moisture and Ocean Salinity (SMOS) mission of the European Space Agency (ESA) (Kerr et al., 2010), and more recently with the launch of the Soil Moisture Passive and Active (SMAP) (Entekhabi et al., 2010) mission of the National Aeronautics and Space Administration (NASA). Based on these data, Level-3 and Level-4 novel products are starting to emerge. In Section 3, the main principles of the algorithm producing the Level-3 CATDS data sets are explained. The Level-3 SMOS products use the L1B Fourier domain brightness temperatures (TB) as main input, but they use the same forward physical model as ESA Level-2 product (Kerr et al., 2012). Therefore, a very short introduction to the main characteristics of the SMOS Level-2 retrievals is also provided. The potential use of SMOS data is exemplified through two applications for drought and flood prediction.

p0030 The third part describes the algorithm of soil moisture estimation for a crucial application, numerical weather prediction (NWP), using both active and microwave remote sensing information. It is expected that the synergetic use of both types of data in land data assimilation systems will support more consistently their influence on forecasts of air temperature and humidity within the boundary layer. Part four presents an overview of the main challenges identified in the delivery of accurate soil moisture data sets based on Earth observation (EO) techniques for operational applications. Finally, part five concentrates in future perspectives aimed at improving modern data sets and their influence in current and future operational applications.

## s0015 2 STATE-OF-THE-ART SOIL MOISTURE RETRIEVALS AND APPLICATIONS BASED ON ACTIVE MICROWAVE DATA

### s0020 2.1 Production of H-SAF Soil Moisture Products

p0035 Within the "Satellite application facility on support to operational hydrology and water management (H-SAF)" project, three satellite-derived soil moisture products, developed by TU-Wien and the European Center for Medium-Range Weather Forecasts (ECMWF) institutes, are delivered in near-real time: (1) large-scale surface soil moisture by radar scatterometer (H07), (2) small-scale surface soil moisture by radar scatterometer (H08), and (3) profile soil moisture index in the roots region by scatterometer data assimilation (H14).

The algorithm for the ASCAT large-scale soil moisture product (H07) was developed by the Vienna University of Technology (TU Wien) and is from its conception a change detection method. As mentioned above, a full description of the algorithm can be found in Wagner et al. (2013). In the context of EUMETSAT's H-SAF, an approach to disaggregate the 25 km ASCAT surface soil moisture data to 1 km using advanced synthetic aperture radar (ASAR) data acquired by the Envisat satellite has been developed. The method exploits the fact that the temporal dynamics of the soil moisture field is often very similar across a wide range of scales; a phenomenon usually referred to as "temporal stability" (Brocca et al., 2014). This means that a linear model may approximate the relationship between local scale and regional scale measurements. In other words, the small-scale surface soil moisture product (H08) is based on the linear disaggregation of the large-scale product (H07), with the regression coefficients constant in time and derived by the combined analysis of ASCAT and ASAR backscatter measurements. Moreover, an ASCAT root-zone soil moisture profile product (H14) has been developed based on ASCAT surface soil moisture data assimilation into the ECMWF extended Kalman filter land surface data assimilation system (de Rosnay et al., 2013). The retrieved ASCAT root-zone soil moisture is an optimal combination between the modeled first guess, the screen-level temperature and humidity analyses, and the ASCAT-derived surface soil moisture, which is propagated forward in time through the root-zone profile. The ASCAT root-zone soil moisture profile product (H14) is available for four soil layers from surface down to 3 m, with a global daily coverage.

## s0025 2.2 Description of the Setup for Flood and Landslides Early Warnings

p0040 In recent years, the Research Institute for Geo-Hydrological Protection (IRPI-CNR) is running some projects with the National Department of Civil Protection and the Regional Department of Civil Protection of Umbria Region for the exploitation of H-SAF soil moisture products for operational floods and landslides monitoring, and prediction, throughout the Italian territory. Specifically, these projects aim at understanding the real potential of satellite soil moisture products for improving the mitigation of the hydrogeological risk, which represents the major climate-related hazard in Italy.

p0045 Before their use within operational systems, satellite soil moisture products need some preprocessing steps to make them suitable for use in hydrological modeling (Brocca et al., 2010). Specifically, the following procedure has been set up for civil protection centers in Italy. First, the three soil moisture products (H07, H08, and H14) are downloaded daily from the H-SAF ftp website and/or the EUMETcast dissemination system. Second, the data are processed to have it ready in a regular grid of ∼10 km horizontal resolution, using the nearest neighbor method. Finally, the products are rescaled, using H14 as reference, with predefined linear relationships to match the temporal mean and variance of each product pixel by pixel.

p0050 Additionally, in central Italy, an advanced monitoring system has been developed in which H-SAF H07 soil moisture product is compared with both in situ and modeled data in real time (see Fig. 1). The combined use of the three data sources allows a robust and reliable assessment of soil moisture conditions that is fundamental for the prediction of the possible occurrence of floods and landslide in the territory (Ponziani et al., 2012; Massari et al., 2014a).

p0055 Two successful examples showing the use of satellite soil moisture data for floods and landslides prediction are described next.

p0060 Recently, Massari et al. (2014a, 2015) have developed a simplified continuous rainfall-runoff model (SCRRM) (see Fig. 2A) that exploits at best satellite soil moisture information, and that is highly suitable for operational applications. Indeed, there is no need for continuous and uninterrupted rainfall and temperature time series as in the standard continuous rainfall-runoff models, and SCRRM is flexible and easy to use. Moreover, the low number of parameters that characterizes SCRRM simplifies its applicability on a large scale and in poorly gaged regions. SCRRM was already applied to a small catchment in Greece by Massari et al. (2014b) in the context of a European project addressed to the development of an early warning system for flood and fire risk assessment and management (http://www.flire.eu/en/). Moreover, SCRRM was applied to 35 basins throughout Italy (Fig. 2) (Massari et al., 2015) with two H-SAF soil moisture products (H07 and H14). The results in terms of flood prediction were satisfactory with mean value of the Nash-Sutcliffe efficiency equal to 0.58 and 0.61 when using H14 and H07 as input, respectively. As a consequence, SCRRM is going to be implemented at a national level for flood prediction in Italy by using the near-real time soil moisture products provided through the H-SAF project.

p0065 The use of satellite soil moisture data for landslide prediction was successfully demonstrated in Brocca et al. (2012). Specifically, the improvements on the prediction of movements of the Torgiovannetto landslide, located near the famous town of Assisi, were investigated. For the period 2007–2009, the landslide movements were recorded for a series of rainfall events thanks to an extensometers network that was established in 2005. Additionally, meteorological data (rainfall and air temperature) and satellite soil moisture data from H07 product were collected for the same period. Meteorological and soil moisture data were used as input into a multiple linear regression model used to predict the observed landslide movements. As shown in Fig. 3, the use of only rainfall information has low potential for estimating landslide movements with a correlation coefficient, $r$, equal to 0.219. However, by including satellite soil moisture data in the regression model, the agreement with the observations is significantly higher with $r=0.821$. On this basis, an operational system was implemented within the Regional Department of Civil Protection of Umbria Region for the monitoring of soil moisture conditions through satellite data (see also Fig. 1) that is currently used for issuing, day-by-day, alerts for the hydrogeological risk.

B978-0-12-803388-3.00018-8, 00018



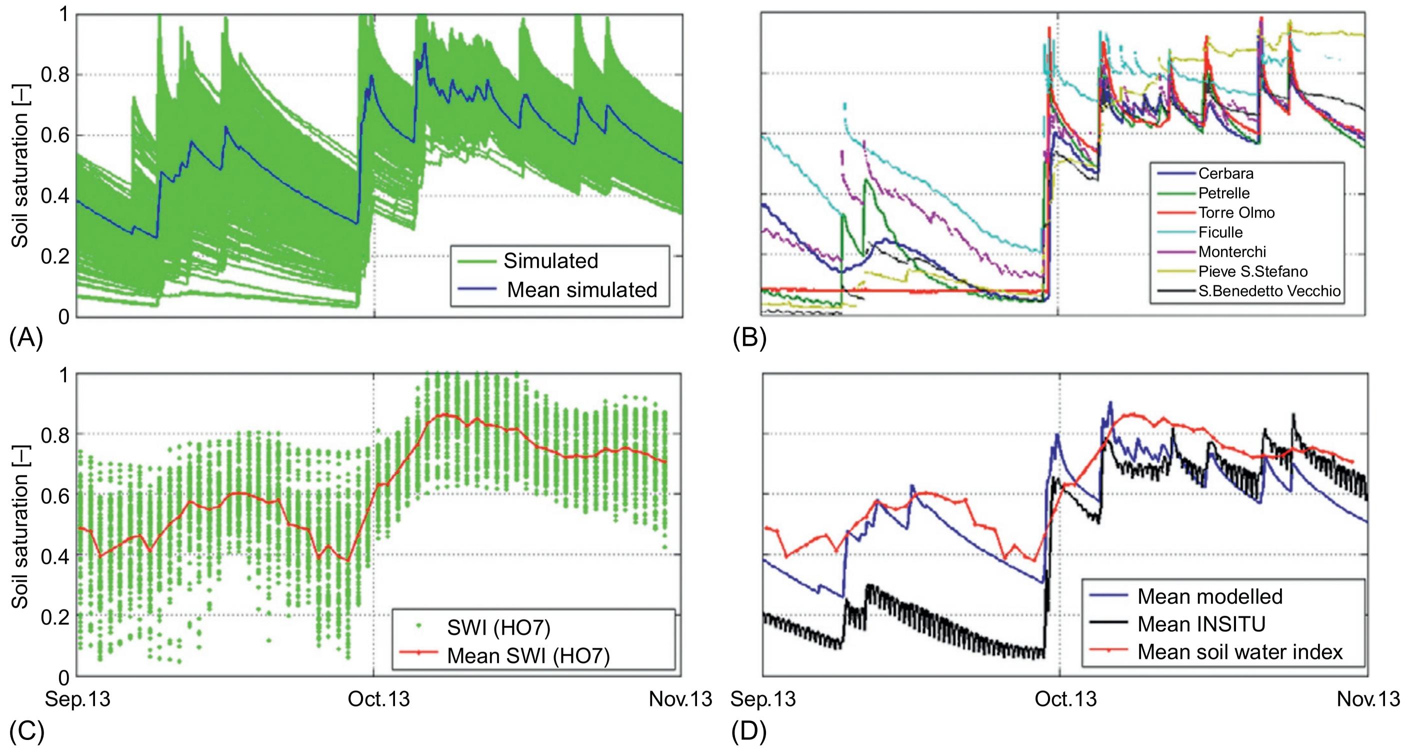


f0010 **FIG. 1** Real-time soil moisture monitoring system implemented for the Umbria Region Civil Protection Centre showing the time series of (A) simulated soil moisture from soil water balance modeling (Ponziani et al., 2012), (B) in situ stations, (C) soil water index (SWI) obtained from H-SAF H07 product, and (D) spatial mean of modeled, in situ, and satellite data. (D) Provides a real-time assessment of average soil moisture conditions in the territory from the three data sources, thus representing a robust estimate to be used for the forecasting of floods and landslides occurrence.

B978-0-12-803388-3.00018-8, 00018



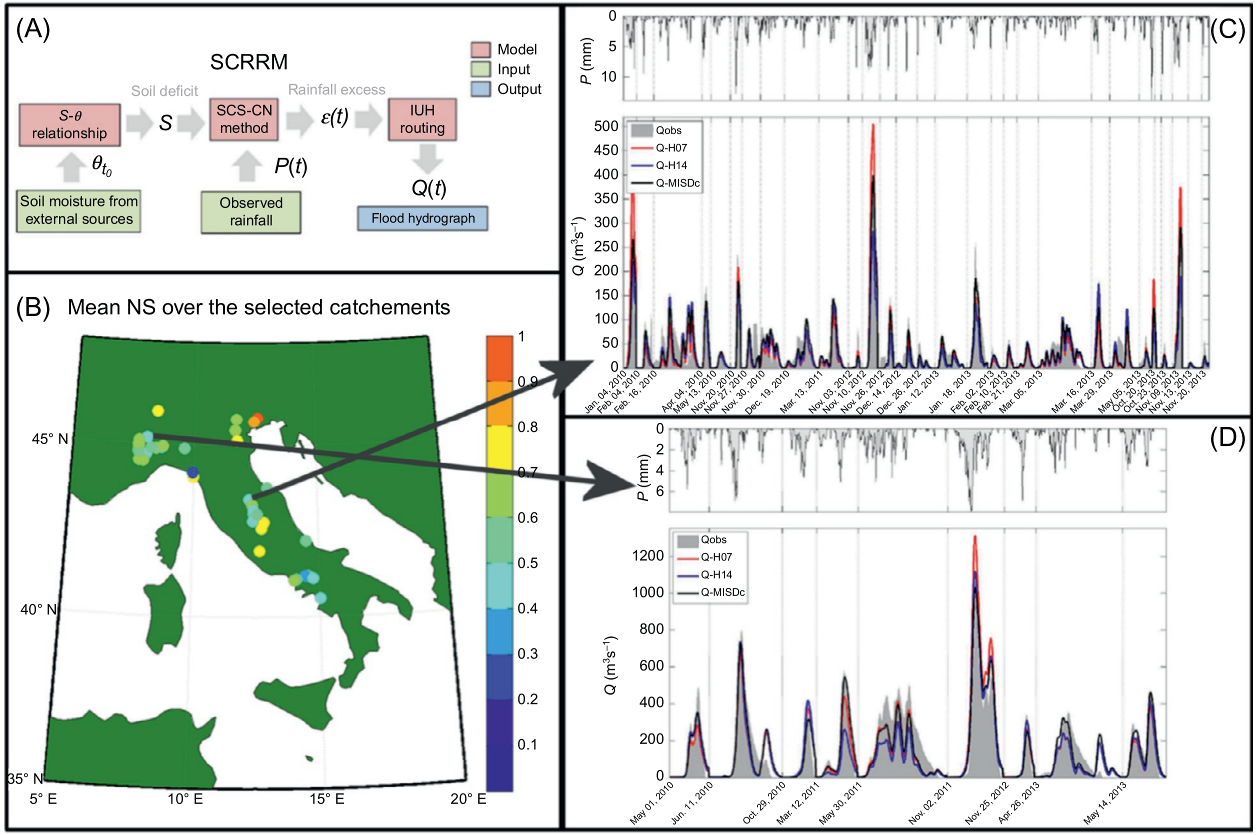


f0015 **FIG. 2** Application of simplified continuous rainfall-runoff model (SCRRM) to 35 basins throughout the Italian territory: (A) structure of SCRRM; (B) map showing the mean Nash-Sutcliffe equation for each basin in terms of flood prediction by using the H-SAF H14 product; (C, D) comparison between observed (Qobs) and simulated (Q-H07, Q-H14, and Q-MISDc) discharge for the flood events that occurred in the period 2010–2013 for (C) the Tevere River at Santa Lucia, and (D) the Po river at Carigliano. Q-H07 and Q-H14 are simulated discharge by using SCRRM with H07 and H14 as input; Q-MISDc is obtained by the application of classical continuous rainfall-runoff modeling (Brocca et al., 2010). The three models are found to be able to capture the flood hydrographs with good accuracy, with small differences among them. *(Adapted from Massari, C., Brocca, L., Ciabatta, L., Moramarco, T., Gabellani, S., Albergel, C., de Rosnay, P., Puca, S., Wagner, W., 2015. The use of H-SAF soil moisture products for operational hydrology: flood modelling over Italy*. Hydrology *2(1), 2–22.)*

B978-0-12-803388-3.00018-8, 00018



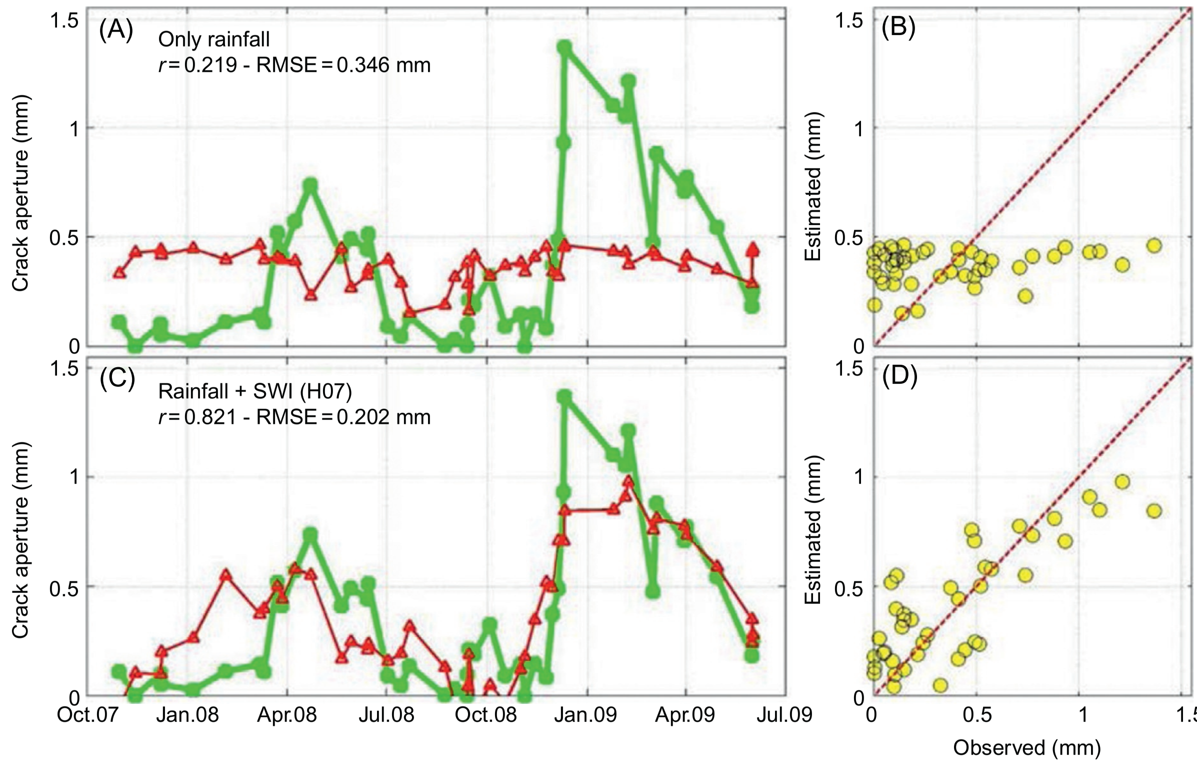


f0020 **FIG. 3** Comparison between observed *(circles)* and estimated *(triangles)* crack aperture for the Torgiovannetto landslide in central Italy as timeseries (A, C) and scatterplot (B, D). Estimated crack aperture are obtained by using a multiple linear regression model that considers (A, B) only rainfall-related quantities (i.e., total rainfall and maximum rainfall for duration of 1 h), (C, D) rainfall and SWI obtained from H-SAF H07 product (*r*, correlation coefficient; *RMSE*, root mean square error). The improvement due to the use of satellite soil moisture data is evident in the bottom panels with an increase in correlation from 0.219 to 0.821. *(Adapted from Brocca, L., Ponziani, F., Moramarco, T., Melone, F., Berni, N., Wagner, W., 2012. Improving landslide forecasting using ASCAT-derived soil moisture data: a case study of the Torgiovannetto landslide in central Italy.* Remote Sens. *4(5), 1232–1244.)*

# s0030 3 STATE-OF-THE-ART SOIL MOISTURE RETRIEVALS AND APPLICATIONS BASED ON PASSIVE MICROWAVE DATA

## s0035 3.1 Multiorbit Soil Moisture Retrieval at SMOS CATDS

### s9000 *3.1.1 Theoretical Basis*

p0070 Level-3 data sets for EO missions are time synthesis products. Data processing of EO missions using multiple revisits of the same area of interest has been widely used in the optical and radar domain. Some examples in the optical domain are the correction of aerosol impact for visible images (Hagolle et al., 2008), the cloud impact correction (Hagolle et al., 2010), and the use of multiple revisits for the land cover classification algorithm (Inglada and Mercier, 2007). With the increase of multitemporal data sets and the open access policy to them, communities in the remote sensing domain are being organized around new approaches for such methodologies. As mentioned previously, the use of multiple revisits in the microwave active domain is common. In the passive microwaves and despite the high potential they have, the majority of operational soil moisture retrieval algorithms are not based on multiple revisits. The main reasons are the wide swath, the coarse resolution, and high revisit time [1 day for AMSR-E (Njoku et al., 2003)], 2–3 days for SMOS (Kerr et al., 2010) and SMAP (Entekhabi et al., 2010).

p0075 Because of its novelty, the basic information in the production of the Level-3 data soil moisture retrievals from the SMOS satellite is provided in this section. The generation is produced at CATDS, a postprocessing center for SMOS data initiated by CNES (Centre National d'Etudes Spatiales). The processing chains running at CATDS do not only produce time synthesis products for the mission in a gridded format but they also take advantage of the frequent revisit of SMOS to make a multiorbit, multiparameter retrieval. The Level-3 processor uses as a forward model the same physical model as the Level-2 processor. A short summary of the model features is provided here. The SMOS Level-2 retrieval can be divided into two major components.

p0080 The first component is a physical model that computes the TB at the antenna reference frame forced by ancillary data and physical parameters value. The selected physical model for the SMOS mission is the L-band microwave emission of the biosphere (L-MEB) (Wigneron et al., 2007) tau-omega model. A comparison of several models used for soil moisture retrieval from microwave sensors is presented in Miernecki et al. (2014). The main features of the L-MEB physical model implementation into the SMOS operational processors are:

u0010 - Single scattering is considered.
u0015 - A combined retrieval of soil moisture and vegetation optical thickness in nominal surfaces by use of angular signature information.
u0020 - Dual polarization is modeled; full polarization is used only to take into account the Faraday rotation and the geometric rotation to change the reference frame.

B978-0-12-803388-3.00018-8, 00018



u0025 - Consideration of antenna patterns (weighting function) change due to the acquisition configuration and mean antenna pattern (ATBD L2). Fig. 4 (from Al Bitar et al., 2012) shows the mean weighting function and its associated cumulative normalized function. The mean weighting function expresses the average contribution with respect to the distance. The cumulative function expresses how much of the signal is contained in a disc of given radius. For example, at ~20 km radius, the 0.5 coefficient corresponds to 3 dB noise level and about 86% of the signal if a homogeneous surface is considered. This corresponds to the nominal resolution of the sensor.

u0030 - Surface heterogeneity is considered through aggregated land cover at 4 km. The contributions are then aggregated based on the mean antenna pattern. An area of 125 km by 125 km is considered at each retrieval node, ensuring that the complete surface is covered.

u0035 - Dynamic changes in surface heterogeneity are considered through the use of weather data from ECMWF.

p0115 Since the mission launch many modifications have been applied to the operational processing model either through improved parameterization (Rahmoune et al., 2014) or through the choice of physical models (Mialon et al., 2015).

p0120 The second component is an optimization scheme that minimizes a Bayesian cost function, thus minimizing the differences between the observed TB and the modeled one while retrieving the physical parameter values. Adding to the previous components a series of preprocessing and postprocessing steps makes it possible to filter the input data for undesired effects, like the decrease of quality due to spatial sampling or radio frequency interference (RFI) (Oliva et al., 2012; Richaume et al., 2014).

p0125 The physical approach conducted at Level-3 is the same one as for Level-2. In fact at the core of the processing the same implementation for the physical

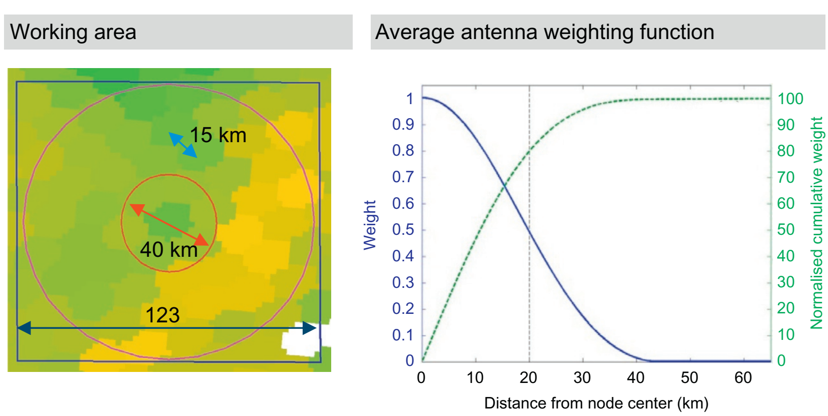


f0025 **FIG. 4** Working area *(left)* and weighting coefficient of the synthetic antenna as a function of distance.

B978-0-12-803388-3.00018-8, 00018



model is used. The main difference in Level-3 is the use of several orbits to retrieve soil moisture. This has an impact on the postprocessing steps for selecting the orbits and the optimization scheme to retrieve the parameters. Because Level-2 retrieval is a multiparameter retrieval, Level-3 is then a multiorbit, multiparameter retrieval. The reasons that motivate the use of the multiorbit approach are the following:

u0040 • The angular sampling of a radiometric accuracy at the border of the swath is reduced, and using a multiorbit approach can help to improve the number of successful retrievals at the border.

u0045 • It is expected that the vegetation optical depth change between consecutive retrievals at ascending or descending passes separately is highly correlated. In fact, in the microwaves domain, the vegetation optical depth is mainly correlated to the vegetation water content, which, in turn, is correlated to the leaf area index (LAI).

p0140 Other general motivations for Level-3 products are to provide a gridded product, in contrast to swath-based products, more adapted for the scientific community, and to provide products at 25 km sampling more consistent with the sensor nominal resolution.

### s0040 3.1.2 Orbit Selection

p0145 The previous motivations guided the elaboration of the retrieval algorithm. First, the following criteria are applied for the selection of revisits:

u0050 • Ascending and descending orbits processing are completely separated.

u0055 • TB products are produced. In fact, this is equivalent to a rerun of the last step of the Level-1 processing chain to make the transition from the Fourier domain to the spatial domain based on the new grid.

u0060 • TB products are filtered at high altitudes where more than one revisit occurs to select a revisit per day (latitudes above 60°N and S). The selection criterion is the minimum distance from the center of the swath. The criterion is applied for each grid node.

u0065 • For each day, a 7-day period is considered for each node. Three revisits are considered independently for each grid node. One for the central date, one for the 3.5 days before, and one for the 3.5 days after. The selection is made based on minimum distance from the swath center (see Fig. 5).

### s9005 3.1.3 Retrieval Algorithm

p0170 As a result of applying the previous steps, observed TB at the antenna reference frame are obtained. A Bayesian cost function that includes multiorbits information is constructed. This is achieved by incorporating in the retrieval approach a temporal autocorrelation function of the retrieved parameters (in this case the vegetation optical depth). The cost function becomes

B978-0-12-803388-3.00018-8, 00018



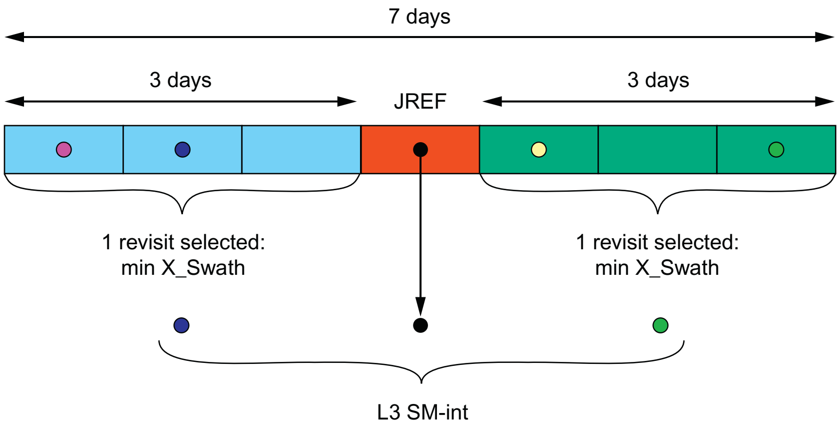


f0030 **FIG. 5** Selection of revisit orbits for the multiorbit retrieval at SMOS CATDS.

$$\mathrm{Cost} = (\mathrm{TB_M} - \mathrm{TB_F})^t \cdot [\mathrm{Cov_{TB}}]^{-1} \cdot (\mathrm{TB_M} - \mathrm{TB_F}) + (P - P_0)^t \cdot [\mathrm{Cov}_P]^{-1} \cdot (P - P_0)$$

where $\mathrm{Cov_{TB}} - \sigma^2_{\mathrm{TB}}$ is the error covariance matrix of TB data assuming no temporal correlation. For vegetation optical depth the error covariance matrix term (considering temporal autocorrelation and no cross correlation between the different parameters) is defined as

$$\mathrm{Cov}_{P_i} = \sigma^2_{i0}(t_1) \cdot \begin{pmatrix} 1 & \rho_i(t_1, t_2) & \cdots & \rho_i(t_1, t_{\mathrm{NV}}) \\ \rho_i(t_1, t_2) & 1 & \cdots & \cdots \\ \cdots & \cdots & 1 & \cdots \\ \rho_i(t_1, t_{\mathrm{NV}}) & \cdots & \cdots & 1 \end{pmatrix}$$

and for all other parameters $\mathrm{Cov}_{P_i} = \sigma^2_{i0}(t_n) \cdot I$. The vegetation optical thickness correlation is modeled with a Gaussian autocorrelation function:

$$\mathrm{Correl_{Tau}}(t_1, t_2) = \mathrm{Corr_{max}}(t_1, t_2) \cdot \exp\left(-\frac{(t_1 - t_2)^2}{\mathrm{Tc}^2}\right)$$

where

- u0070 $t_1$ and $t_2$ are the time (expressed in days) corresponding to the vegetation optical thickness retrievals,
- u0075 $\mathrm{Corr_{max}}(t_1, t_2)$ is the maximum amplitude of the correlation function between $t_1$ and $t_2$,
- u0080 Tc is the characteristic correlation time for the vegetation optical thickness Tau, and
- u0085 Tc = 30 days for forests and Tc = 10 days for low vegetation.

**B978-0-12-803388-3.00018-8, 00018**



p0195 Starting from daily maps, time synthesis products (3 days, 10 days, and monthly) are then provided. A detailed description of the algorithm with corresponding products is presented in Kerr et al. (2013). CATDS products are produced at iFremer for CNES, and they are accessible through the website: http://www.catds.fr. Fig. 6 shows the median soil moisture for the month of Sep. obtained from the SMOS L3 soil moisture products from 2010 to 2016.

## s0045 3.2 Root-Zone Soil Moisture and Application for Drought Monitoring

p0200 Level-4 products are high-end products derived from lower-level products in combination with models and ancillary data. Root-zone soil moisture can be accessed from surface soil moisture either by the use of a land data assimilation system or by the use of empirical approaches. Root-zone soil moisture is the primary variable in the monitoring of agricultural drought. At CATDS, a data-driven approach is used to compute the root-zone soil moisture. Wagner et al. (1999) suggested the use of an exponential filter to access root-zone soil moisture from shallow soil moisture. Albergel (2008) provided a sequential formulation of the model and tested it over local sites in the southwest of France. Qiu et al. (2014) showed that surface soil moisture can be considered as a reliant proxy to root-zone soil moisture. At SMOS CATDS Level-4, root-zone soil moisture is provided by applying the exponential filter in combination with the Food and Agriculture Organization (FAO, United Nations) method FAO56, the latter used to compute the transpiration in a deeper soil layer (10 cm to 1 m).

p0205 The water availability in the root-zone is computed using a double bucket hydrological model. The model is forced only by surface soil moisture and no precipitation data is used. The main remote sensing data used is the SMOS L3 CATDS retrieved soil moisture. The MODIS NDVI is used to compute vegetation transpiration rates. The other ancillary data sources are operational climate analysis data from the National Centers for Environmental Prediction (NCEP), soil texture from FAO, and surface cover from ECOCLIMAP-II.

### s0050 *3.2.1 From Near-Surface to the 20 cm Layer*

p0210 The surface layer extending from the 0–20 cm is the place where complex processes like infiltration, runoff, percolation, and evaporation take place. It is possible to parameterise a global model at 25 km resolution taking into consideration all those processes, but the uncertainty associated with the parameters will be high. For this reason a simple water budget model is used (also referred to as exponential filter) to compute the water content in the 0–20 cm layer. The sequential formulation of the exponential filter presented by Albergel (2008) is used. The only parameter needed is the time lag in days that defines the rate of transfer of the water to deeper layers. This simple formulation has been developed for microwave remote sensing data and is well adapted for SMOS data.

**Srivastava, 978-0-12-803388-3**

B978-0-12-803388-3.00018-8, 00018



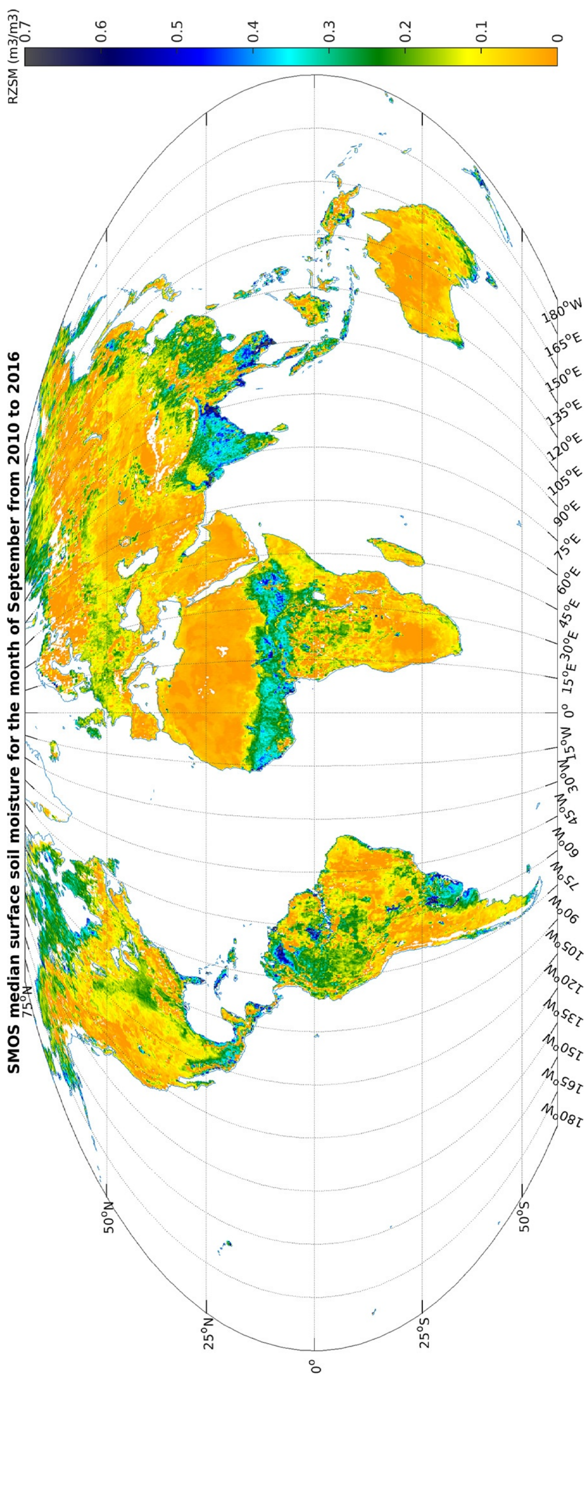


f0035 **FIG. 6** Median soil moisture during the month of Sep., from 2010 to 2016, using the multiorbital retrieval from CATDS.

Srivastava, 978-0-12-803388-3

B978-0-12-803388-3.00018-8, 00018



### s0055 3.2.2 From the 20 cm Layer to the Root-Zone Layer

p0215 The layer of interest for drought is the 0–200 cm layer. The exponential filter used in the previous layer is not adapted to take into account the vegetation transpiration and it does not take into account capillary rise. For this reason, a budget model based on a linearized Richards equation formulation is selected for the second layer. The transpiration rate of the vegetation is computed by Au6 means of the FAO method (Allen, 1998). Two types of data are needed to drive the transpiration: the LAI of the vegetation and climatic data to compute potential leaf transpiration. The NDVI is obtained from the 16-days global MODIS data interpolated over the EASE 25 km grid. The climate data are downloaded through NCEP servers. These data are interpolated to the SMOS product grid and used to compute the potential transpiration.

p0220 As mentioned above, the root-zone soil moisture can be used to monitor the agricultural drought. Fig. 7 shows the status of the root-zone soil moisture for Jul. 15, 2012, obtained from SMOS CATDS processing.

### s0060 3.2.3 Case of the Horn of Africa 2011 Droughts

p0225 Fig. 8 shows the root-zone soil moisture index from SMOS for Oct. 2011 over Africa. This index varies between 0 for dry conditions and 1 for wet conditions. The soil moisture is considered as equal to wilting point during dry conditions and to field capacity during wet conditions. It shows the extent of the droughts over the horn of Africa. The wet conditions over the western part of the Sahel are also clearly visible. An extraction of the root-zone soil moisture during the dry season corresponding to the Sahel transition region, between latitudes 9°S and 22°N, is shown at the bottom of Fig. 8. The figure clearly depicts the wet conditions in the interior Niger Delta and in the south of Sudan, which is a highly irrigated agricultural area. This shows the potential of a soil moisture-based index to monitor not only drought due to rainfall deficit but also vegetation stress due to irrigation deficit at regional scale.

## s0065 4 STATE-OF-THE-ART SOIL MOISTURE ANALYSIS FOR NWP

p0230 Soil moisture accurate initialization in NWP models is crucial for good quality forecasts from short to medium ranges (Beljaars et al., 1996; Douville et al., 2000; Drusch and Viterbo, 2007). Due to the long memory of the soil moisture reservoir, its influence can be extended from monthly to subseasonal time scales (Koster et al., 2011; Dirmayer, 2000; Ni-Meister et al., 2005). During many years and due to the lack of satellite data, soil moisture has been constrained with in situ observations of air temperature and humidity from the SYNOP network, preventing in this way model drifts toward unrealistic states of the soil. The ingestion of the soil moisture information contained in screen-level variables has been carried out with a land data assimilation system (LDAS). The core of the ECMWF soil moisture analysis is a point-wise simplified extended Au7 Au8

B978-0-12-803388-3.00018-8, 00018



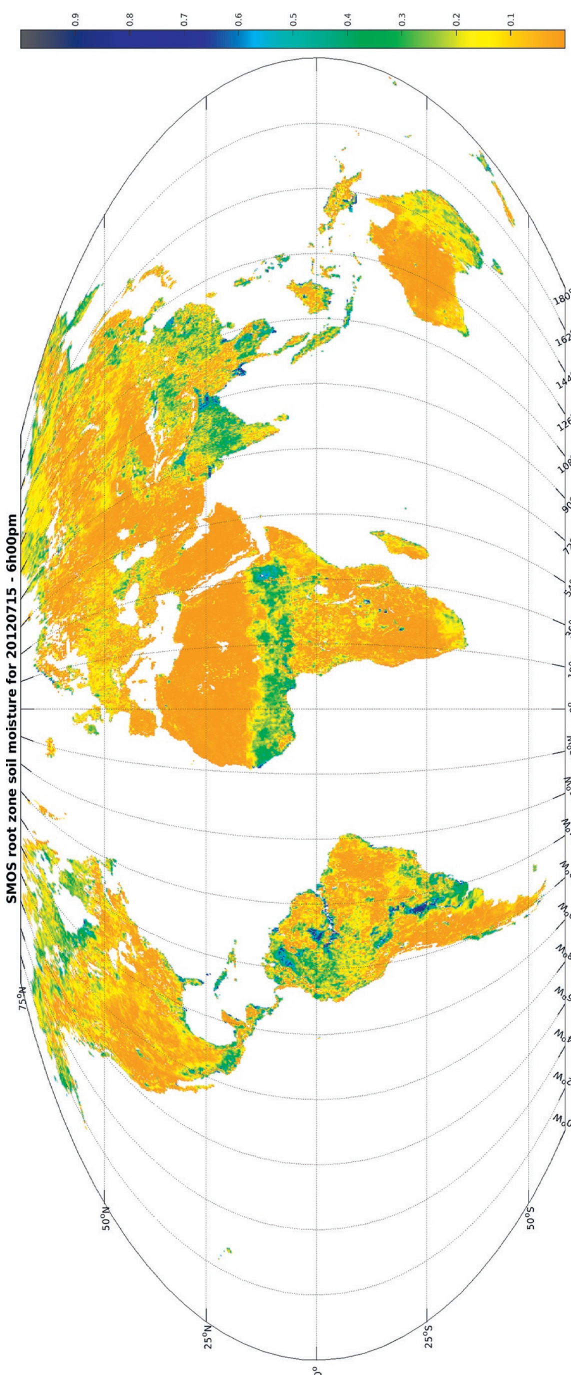


f0040 **FIG. 7** Root-zone soil moisture index map for Jul. 15, 2012, obtained from the SMOS CATDS processing.

B978-0-12-803388-3.00018-8, 00018



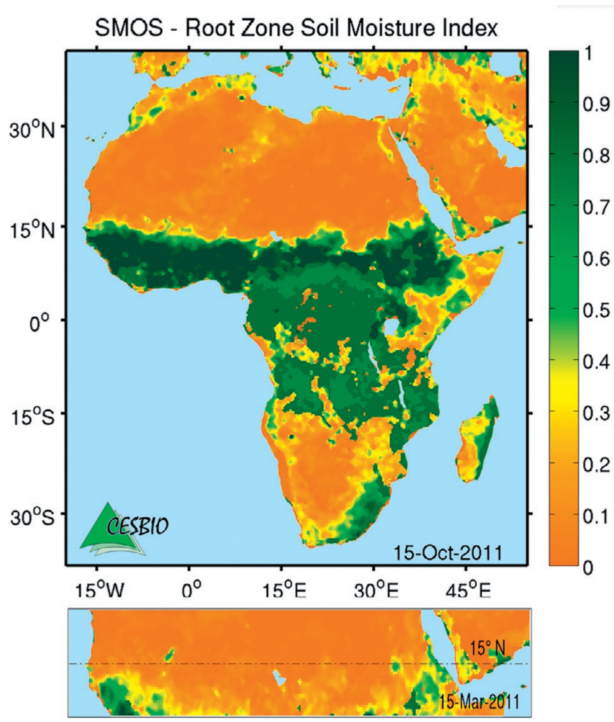


f0045 **FIG. 8** The top panel shows the root-zone soil moisture index over Africa for Oct. 15, 2011. The droughts over the horn of Africa can be clearly observed. The bottom panel shows the soil moisture conditions over the Sahel region during the dry season. The wet areas of the internal Niger Delta and the South Khartoum agricultural area can be clearly observed.

Kalman filter (SEKF) (Drusch et al., 2009a; de Rosnay et al., 2012), which is a data assimilation scheme particularly suitable for low-dimensional problems, as the ECMWF soil moisture analysis. At each ECMWF 12-h assimilation cycle and for each model grid point the SEKF computes soil moisture increments for the top three soil layers of the hydrology tiled ECMWF scheme of Surface Exchanges over land (HTESSEL) (Balsamo et al., 2009). The objective is producing small corrections of the model forecasted value consistent with the observations. Soil moisture increments ($\Delta\mathbf{sm}$) are computed at analysis time ($t_a$) based on the misfit between observations ($\mathbf{y}^o$) and the model equivalent of the observations ($H_i(\mathbf{x}^b)$) at the time of the observations ($t_i$), also called innovation vector. The uncertainty of the forecast soil moisture value and the observations are also accounted for explicitly in the background error covariance matrix **B** and in the observation error covariance matrix **R**, respectively. Soil moisture increments are calculated as

$$\Delta\mathbf{sm}(t_a) = \mathbf{K}_i\left[\mathbf{y}^o(t_i) - H_i\left(\mathbf{x}^b\right)\right]$$

being

$$\mathbf{K}_i = \left[\mathbf{B}^{-1} + \mathbf{H}_i^{\mathrm{T}}\mathbf{R}^{-1}\mathbf{H}^{\mathrm{T}}\right]^{-1}\mathbf{H}_i^{\mathrm{T}}\mathbf{R}^{-1}$$

the Kalman gain, which modulates the amount of correction of the background soil moisture value. $H_i$ is the forward observation operator bringing observations and model equivalents to the same space for comparison purposes. In the case of brightness temperatures, $H_i$ is the radiative transfer model (RTM) that simulates TB at the top of the atmosphere as a function of soil initial states. The ECMWF RTM for low frequencies passive microwaves is the community microwave emission model (Drusch et al., 2009b; de Rosnay et al., 2009; Muñoz-Sabater et al., 2011). The linearized version of $H_i$ is the Jacobian of the observation operator and is represented by $\mathbf{H}_i$. It estimates the sensitivity of the model equivalent of the observations to individual perturbations of the model state vector by a small amount. For each element of the control state vector, a perturbed model integration is required; this being the main driving cost of the SEKF in the operational system. The greater the confidence about the observations, the more weight the assimilated observations will have in the computed soil moisture increments. Au9

p0235 The current ECMWF operational system uses 2 m temperature and relative humidity analysis as input for the observation vector (available at synoptic times), and since recent dates soil moisture index observations from the ASCAT active system. The ECMWF operational soil moisture analysis also includes the possibility of using L-band TB from the SMOS passive system (Muñoz-Sabater, 2015), alone or in combination with screen-level variables and ASCAT soil moisture retrievals. The soil moisture background errors of the three top soil layers of the HTESSEL model are currently fixed and static during the assimilation window. The standard deviation of these variables is assumed to be $\sigma_{\mathrm{sm}} = 0.01\ \mathrm{m}^3\ \mathrm{m}^{-3}$. The operational observation errors in the **R** matrix are also fixed and account for the standard deviation of 2 m temperature, relative humidity, and ASCAT soil moisture observations. Since May 2015, these values were reviewed and set, respectively, to $\sigma_{\mathrm{T}} = 1$ K, $\sigma_{\mathrm{RH}} = 4\%$, and $\sigma_{\mathrm{ASCAT}} = 0.05\ \mathrm{m}^3\ \mathrm{m}^{-3}$. The observation error for SMOS TB is currently being optimized. It has the advantage that is specific to each observation, with a minimum value equivalent to the radiometric accuracy, making the SMOS TB uncertainty more objective than a constant fixed value. Fig. 9 shows an example of accumulated soil moisture increments obtained by assimilating screen-level variables and SMOS TB observations.

p0240 The contribution of ASCAT soil moisture retrievals for better initialization of soil moisture in the ECMWF atmospheric system was studied first by Scipal et al. (2008). In their experiment they used a nudging scheme to assimilate ASCAT data; however, compared to the operational optimal interpolation scheme, the use of scatterometer data slightly degraded the forecast scores. More recently, de Rosnay et al. (2012) matched the climatology of ASCAT soil

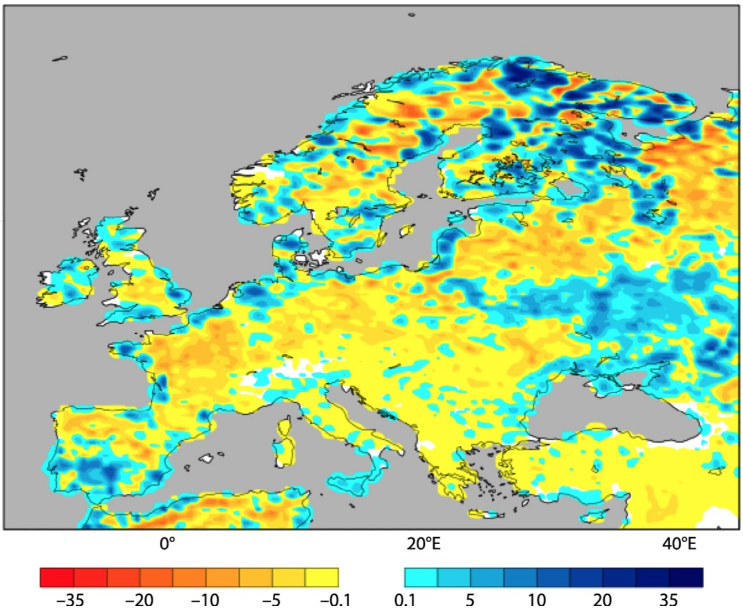


f0050 **FIG. 9** Accumulated soil moisture increments for Jun. 2010 in mm, after combined assimilation of screen-level variables ($T_{2m}$ and $RH_{2m}$) and SMOS TB.

moisture data to that of the ECMWF model through CDF matching and used a SEKF to assimilate the scatterometer data. The new soil moisture state did not improve the correlation with ground validation data significantly. However, improvement in the model, in the bias correction methodology, and in the quality of the scatterometer data from MetOp-B has optimized the use of ASCAT soil moisture retrievals for short-range forecasts.

p0245 Muñoz-Sabater (2015) has shown that the assimilation of SMOS TB in the ECMWF soil moisture analysis typically reduces the amount of water stored in the soil. The negative sign of the soil moisture increments points in the right direction, as they partially correct for a wet bias associated with ECMWF's land surface scheme. Compared to screen-level variables, the assimilation of SMOS TB produces large corrections of soil moisture, which is a combination of the large sensitivity of SMOS data to soil moisture variations, and the larger weight given to the SMOS observations in the LDAS compared to screen variables. An exhaustive validation against more than 400 in situ stations distributed around the world in summer 2010 showed that SMOS observations are especially informative of the soil moisture content in semiarid climates. However, the information provided by screen-level variables, in combination with SMOS TB, has been demonstrated to be especially valuable in temperate climates. Concerning the implications for the forecast of atmospheric variables, the impact of the new soil moisture state due to the joint assimilation of screen-level variables and

SMOS data showed very little impact in 2 m temperature, air temperature, and relative humidity. Larger impact was observed at specific regions, with mixed signs depending on the geographical location. This result may evidence an over-tuning of the parameters controlling coupling processes at the soil-atmosphere interface.

p0250 Despite the preliminary findings above, two aspects should be taken into consideration. First, an optimization of the SMOS observation weight in the land data assimilation system, as well as the revision of other parameters of the soil moisture analysis, will likely produce an updated picture of the real impact of the use of SMOS observations for soil moisture initialization in a weather forecasting model. And second, the combination of SMOS and ASCAT data (as planned to be integrated in the operational system) may solve some of the deficiencies of using only a single type of observation for soil moisture updates.

## s0070 5 OBSTACLES IN THE PRODUCTION OF SOIL MOISTURE RETRIEVALS AND ITS APPLICATIONS

p0255 The production of accurate soil moisture retrievals based on EO-based techniques is a crucial requirement for their use in operational applications. This chapter has inspected the fundaments of the algorithms producing SMOS soil moisture retrievals, for Level-3 and Level-4, the latter being more adapted to end-user applications. It also has presented the use of state-of-the-art soil moisture retrievals and analyses based on both active and passive microwave data sets for hydrological and meteorological applications. The continuous availability and production of such data sets is essential for operational applications. However, several external factors can hamper their production. One of them is the contamination of the geophysical signal by RFI (Njoku et al., 2005; Oliva et al., 2012; Soldo et al., 2015). This is critical in passive L-band, where the level of observed energy is very low. Indeed, some areas across the globe see the number of retrievals strongly reduced by RFIs, resulting in large gaps in given regions, and as a consequence limiting their use for land applications. Retrievals under dense forests are also another challenging area because of the high attenuation of the soil emission. The lack of long L-band time series has prevented large-scale applications that depend on historical data sets. It is expected that the integration of soil moisture data sets from L-Band observations into the ESA climate change initiative (CCI) soil moisture essential climate variable (ECV), a consistent multisensors soil moisture data set will be available in the near future.

p0260 Another issue frequently neglected is the indirect connection existent between soil moisture and the noncontinuous nature of the observations. Soil moisture retrievals may be inconsistent with model simulations, as they may utilize different land surface parameters and background information including soil texture, surface temperature, and vegetation. In fact, soil moisture retrieval involves a prior estimate, frequently from a model. Errors of the prior estimate are often correlated to the background value, and they are commonly not taken into account. These reasons, along with the faster availability of the data, are arguably important reasons to consider the use of direct TB in assimilation schemes for NWP systems (Muñoz-Sabater, 2015), and they have to be carefully considered to produce high-quality soil moisture data sets.

p0265 Despite the obstacles mentioned above, satellite soil moisture products have reached a good level of accuracy and maturity, especially those based on longer time series with active observations. However, their use for operational hydrological applications is still very limited. The main difficulty is due to the spatial mismatch between the resolution of current satellite soil moisture products (from ~400 to ~1500 km$^2$) and the study area under investigation (frequently below 100 km$^2$). Some authors have already demonstrated that even coarse-resolution soil moisture products can still provide useful information for improving runoff and landslide prediction, even for small to medium basins/areas (e.g., Brocca et al., 2010, 2012). The modeling of land surface physical processes is evolving at a faster pace than the resolution at which satellite retrievals are being improved. This tendency will not change in the years to come, likely decades. Therefore, if satellite soil moisture retrievals are intended for use in the new wave of operational applications demanding high-resolution information of soil variables, this mismatch has to be addressed (Wood et al., 2011). Downscaling coarser remote sensing observations to the model resolution, using a set of fine resolution auxiliary data (Merlin et al., 2010; Piles et al., 2011), is one of the most accepted methods used today. Even some recent studies claim the downscaled approach to be carried out with implicit bias correction (Verhoest et al., 2015). The reverse approach consists of upscaling model outputs to the satellite footprint resolution (Crow et al., 2012). The challenge is even greater if different types of data sets at different spatial resolutions and revisit time are intended to be used simultaneously, as it is for the case explained in Section 6. In this case some compromises may be necessary. For example, Fascetti et al. (2016) compared different sources of soil moisture retrievals with Au10 very different characteristics (spatial resolution, observation time, units). The comparison was only possible by means of several assumptions, as the rescaling of the active source of soil moisture retrievals or the spatial collocation through the nearest neighbor approach. They concluded that the way the active data is rescaled has an impact on the comparison results.

p0270 The exploitation of spaceborne observations in land applications is also limited by the shallow penetration depth (~1–5 cm), which is significantly lower than the effective depth at which hydrological or meteorological applications need to extract information from. But even this shallow information can be physically propagated at deeper layers by means of data assimilation methods (Houser et al., 1998; Walker et al., 2001; Muñoz-Sabater et al., 2007, 2008) or by empirical approaches, such as that used in Wagner et al. (1999) and Al Bitar et al. (2013).

p0275 The constant presence of biases is another important element hindering the efficient exploitation of soil moisture retrievals for a wide range of applications. Biases are the cause of systematic differences between the statistical moments of the retrievals and the models. One reason is the fact that while satellite instruments provide an averaged measurement of a shallow layer of the surface, models estimate the numerical value of a prognostic variable over a smaller area but representative of a deeper thickness. The use of different modeling and/or observational approaches typically leads to predictions with different systematic relationships to the assumed truth. Simplifications in the model parameterization and in the retrieval algorithm are also sources of biases. Prior to the joint use of soil moisture retrievals and models, biases should be removed. A popular technique used to remove biases consists of matching the statistical moments of two independent distributions, also called cdf-matching. Frequently, the observations climatology is matched to that of a model equivalent. The remaining disagreement between the "unbiased" observations and the model counterpart contains useful information to constrain the time-space evolution of modeled soil moisture. Although this technique is based on the availability of long time series, several authors have found this technique to work even for short records of satellite data (Reichle and Koster 2004). Other strategies of bias correction methods use least squares regression techniques (Crow et al., 2005; Crow and Zhan, 2007) or variance-based techniques as triple collocation analysis (Stoffelen, 1998). However, one should bear in mind that in reality, even if the model and observations are subjected to a bias correction approach, residual biases frequently remain in the systems. Au11

p0280 A final important issue to consider is the format and the data volume (Muñoz-Sabater et al., 2012). Indeed, end-users are frequently uncomfortable working with large data sets and with unconventional data formats. Even though it may look like a negligible problem, this is still today one of the major obstacles for the effective use of satellite soil moisture data in several operational domains. Therefore, it is advisable to invest in capacity building for making, on one hand, the satellite products more user-friendly and, on the other hand, the possible users aware of the large potentials that these products can offer.

p0285 In the production of continuous, high-quality, and useful soil moisture data sets for operational use, the above are not the only obstacles and caveats to be taken into account, yet they are common to all soil moisture retrievals algorithms and they need to be addressed for each specific application.

## s0075 6 FUTURE OUTLOOK

p0290 Soil moisture data sets based on EO techniques have brought a lot of benefit to a wide range of daily applications such as those shown in this chapter, and many others such as fire risk assessment and water resources management of agricultural water monitoring. The observed benefits should encourage us to carry out more investigations to foster the use of satellite soil moisture data in different communities (hydrology, geomorphology, agriculture, etc.).

p0295 With the purpose of improving the accuracy of satellite rainfall products, some approaches using satellite soil moisture data were recently developed (Crow et al., 2009; Pellarin et al., 2013; Brocca et al., 2013; Wanders et al., 2015). Among them, Brocca et al. (2013) proposed a new method for estimating rainfall using soil moisture observations, called SM2RAIN. The method is based on the inversion of the soil water balance equation; that is, it estimates the rainfall by using the change in time of the amount of water stored into the soil, thus considering the "soil as a natural rain gage." SM2RAIN has been applied both on a local (Brocca et al., 2013, 2015) and on a global scale (Brocca et al., 2014) with ground and satellite soil moisture data as input with satisfactory results in terms of rainfall estimation. Moreover, Massari et al. (2014b) and Ciabatta et al. (2015b) found that the correction of rainfall through SM2RAIN provides improvement in flood modeling when compared to the use of rain gage observations only.

p0300 On this basis, in the next phase of the H-SAF project, the development of a new precipitation product in near-real time is expected that integrates satellite soil moisture (through SM2RAIN) and precipitation products. Basically, this new product will integrate the "top-down" and "bottom-up" perspectives for rainfall estimation from remote sensing. The retrieval of rainfall in the state-of-the-art products is based on a "top-down" approach; that is, rainfall is obtained through the inversion of the atmospheric signals scattered or emitted by atmospheric hydrometeors. In the new concept on which the SM2RAIN algorithm was developed, rainfall is obtained in a "bottom-up" perspective from the knowledge of the amount of water stored in the soil and measured from remote sensing. The two perspectives are independent and their integration is capable of providing a higher-quality rainfall product that takes advantage of the benefits of both perspectives. First validation results in Italy have shown highly promising results (Ciabatta et al., 2015a) as the integrated product is found to outperform state-of-the-art products and to provide reliable information for hydrological applications (Ciabatta et al., 2015b).

p0305 Soil moisture is identified as an ESA ECV for climate change studies. It is thus important to have a long (decadal) and consistent data set of soil moisture obtained from multiple EO missions. One of the outcomes of the ESA CCI on soil moisture is a consistent decadal data set of observed surface soil moisture from microwave remote sensing. The second phase of this program will include SMOS data and, eventually, SMAP data will be included too. The overlap of SMOS and SMAP missions will make possible the continuity of L-band observations for soil moisture. With the emergence of the European Copernicus program [previously known as Global Monitoring for Environment and Security (GMES)], synergistic studies between active (Sentinel-1) and passive (SMOS, SMAP) sensors are expected, providing new surface soil moisture products that make use of the advantages of the different sensors to provide a high-temporal (3 days) and high-spatial (100 m) resolution within recommended accuracy. By

B978-0-12-803388-3.00018-8, 00018



associating these products with optical data and crop modeling, new applications related to agricultural management (irrigation, vegetation stress, and others) will be elaborated. A multitude of services is expected to emerge from these activities, accelerating the technological transition from research (and public) to commercial (and private) sectors.

p0310 Soil moisture in fully coupled land-atmospheric systems will require special attention because of the enhanced predictability skill coming from the long memory of the soil moisture reservoir. Soil moisture in NWP systems has been optimized to provide sensible and latent heat fluxes, based on the assimilation of atmospheric temperature and moisture errors in LDAS. The risk is that model errors can be accumulated into soil moisture, with negative effects for the realism of the soil water content. However, the availability of observations from new platforms and the irruption of new applications such as carbon flux modeling and river flow forecasts require high-quality soil moisture, as well as other variables of the water cycle as runoff. In this context, the realism of both the surface processes and the numerical value of surface variables are necessary. The improvement of soil moisture in the future will be supported by a more comprehensive modelization of surface processes, such as the explicit processes of vegetation (Boussetta et al., 2013) and the mutual interaction of the water, energy, and carbon cycles. The use of satellite observations (sensitive only to the top cm of the soil) will be enhanced by increasing the soil vertical discretization, currently composed at ECMWF of four layers at 7, 21, 72, and 189 cm. The benefits of adding extra layers will enhance land-atmosphere interaction, and it will extend the memory from the deeper soil layers and the model capability to represent multiple time scales. In the data assimilation side, the flexible structure of the ECMWF SEKF opens a lot of new opportunities, including the exploitation of new satellite surface products, such as SMAP data, and the extension of the SEKF to analyze additional variables, such as soil temperature, snow temperature, and mass and vegetation parameters.

p0315 This chapter has explained how the use of scatterometer data from ASCAT and radiometric data from SMOS has the potential to produce better, more realistic soil moisture states not only for weather forecasting but also potentially for other applications such as river flood forecasting or carbon sources estimation. Both types of data have already shown, in certain cases, deficiencies in terms of poor impact in the soil moisture analysis or in air temperature and humidity forecasts. Active and passive systems are complementary in many different ways. An upgraded operational version of the ECMWF surface analysis will combine both types of remote sensing information, along with the traditional use of conventional data, overcoming in this integrated way some of the observed deficiencies and at the same time increasing the efficiency of the LDAS.

## ac0010 ACKNOWLEDGMENTS

The authors acknowledge support from EUMETSAT through the “Satellite Application Facility on Support to Operational Hydrology and Water Management” H-SAF project and the

National Department of Civil Protection of Italy. Also, thanks for the support of ESA for the SMOS project at ECMWF. Finally, acknowledgments to CNES and Ifremer for the SMOS CATDS data sets.

## REFERENCES

Al Bitar, A., Leroux, D., Kerr, Y.H., Merlin, O., Richaume, P., Sahoo, A., Wood, E.F., 2012. Evaluation of SMOS soil moisture products over continental US using the SCAN/SNOTEL network. IEEE Trans. Geosci. Remote Sens. 50 (5), 1572–1586.

Al Bitar, A., Kerr, Y., Merlin, O., Cabot, F., Wigneron, J.-P., 2013. Global drought index from SMOS soil moisture. In: IEEE International Geoscience and Remote Sensing Symposium, IGARSS 2013, Melbourne, Australie, 21–26 July.

Albergel, C., Rüdiger, C., Pellarin, T., Calvet, J.-C., Fritz, N., Froissard, F., Suquia, D., Petitpa, A., Piguet, B., Martin, E., 2008. From near-surface to root-zone soil moisture using an exponential filter: an assessment of the method based on in-situ observations and model simulations. Hydrol. Earth Syst. Sci. 12, 1323–1337. http://dx.doi.org/10.5194/hess-12-1323-2008.

Allen, R.G., 1998. Crop Evapotranspiration-Guidelines for Computing Crop Water Requirements-FAO Irrigation and Drainage Paper 56. Food and Agriculture Organization of the United Nations, Rome. No. 6541.

Balsamo, G., Viterbo, P., Beljaars, A., van den Hurk, B., Hirschi, M., Betts, A., Scipal, K., 2009. A revised hydrology for the ECMWF model: verification from field site to terrestrial water storage and impact in the integrated forecast system. J. Hydrometeorol. 10, 623–643.

Beljaars, A.C.M., Viterbo, P., Miller, M., 1996. The anomalous rainfall over the United States during July 1993: sensitivity to land surface parameterization and soil moisture anomalies. J. Hydrometeorol. 124, 362–383.

Boussetta, S., Balsamo, G., Beljaars, A., Agusti-Panareda, A., Calvet, J.-C., Jacobs, C., van den Hurk, B., Viterbo, P., Lafont, S., Dutra, E., Jarlan, L., Balzarolo, M., Papale, D., van der Werf, G., 2013. Natural carbon dioxide exchanges in the ECMWF integrated forecasting system: implementation and offline validation. J. Geophys. Res. 118, 1–24. http://dx.doi.org/10.1002/jgrd.50488.

Brocca, L., Melone, F., Moramarco, T., Wagner, W., Naeimi, V., Bartalis, Z., Hasenauer, S., 2010. Improving runoff prediction through the assimilation of the ASCAT soil moisture product. Hydrol. Earth Syst. Sci. 14, 1881–1893.

Brocca, L., Ponziani, F., Moramarco, T., Melone, F., Berni, N., Wagner, W., 2012. Improving landslide forecasting using ASCAT-derived soil moisture data: acase study of the Torgiovannetto landslide in central Italy. Remote Sens. 4 (5), 1232–1244.

Brocca, L., Melone, F., Moramarco, T., Wagner, W., 2013. A new method for rainfall estimation through soil moisture observations. Geophys. Res. Lett. 40 (5), 853–858.

Brocca, L., Zucco, G., Mittelbach, H., Moramarco, T., Seneviratne, S.I., 2014. Absolute versus temporal anomaly and percent of saturation soil moisture spatial variability for six networks worldwide. Water Resour. Res. 50 (7), 5560–5576.

Brocca, L., Massari, C., Ciabatta, L., Moramarco, T., Penna, D., Zuecco, G., Pianezzola, L., Borga, M., Matgen, P., Martínez-Fernández, J., 2015. Rainfall estimation from in situ soil moisture observations at several sites in Europe: an evaluation of SM2RAIN algorithm. J. Hydrol. Hydromech. 63 (3), 201–209.

Ciabatta, L., Brocca, L., Massari, C., Moramarco, T., Gabellani, S., Puca, S., Wagner, W., 2015a. Rainfall-runoff modelling by using SM2RAIN-derived and state-of-the-art satellite rainfall products over Italy. J. Appl. Earth Observ. Geoinf. http://dx.doi.org/10.1016/j.jag.2015.10.004.

Ciabatta, L., Brocca, L., Massari, C., Moramarco, T., Puca, S., Rinollo, A., Gabellani, S., Wagner, W., 2015b. Integration of satellite soil moisture and rainfall observations over the Italian territory. J. Hydrometeorol. 16 (3), 1341–1355.

Crow, W.T., Zhan, X., 2007. Continental-scale evaluation of remotely sensed soil moisture products. IEEE Geosci. Remote Sens. Lett. 4, 451–455.

Crow, W.T., Bindlish, R., Jackson, T.J., 2005. The added value of spaceborne passive microwave soil moisture retrievals for forecasting rainfall-runoff partitioning. J. Geophys. Res. 32. http://dx.doi.org/10.1029/2005GL023543.

Crow, W.T., Huffman, G.F., Bindlish, R., Jackson, T.J., 2009. Improving satellite rainfall accumulation estimates using spaceborne soil moisture retrievals. J. Hydrometeorol. 10, 199–212.

Crow, W.T., Berg, A.A., Cosh, M.H., Loew, A., Mohanty, B.P., Panciera, R., de Rosnay, P., Ryu, D., Walker, J.P., 2012. Upscaling sparse ground-based soil moisture observations for the validation of coarse-resolution satellite soil moisture products. Rev. Geophys. 50. http://dx.doi.org/10.1029/2011RG000372.

de Rosnay, P., Drusch, M., Boone, A., Balsamo, G., Decharme, B., Harris, P., Kerr, Y., Pellarin, T., Polcher, J., Wigneron, J.P., 2009. AMMA land surface model intercomparison experiment coupled to the community microwave emission model: ALMIP-MEM. J. Geophys. Res. 114.

de Rosnay, P., Balsamo, G., Albergel, C., Muñoz-Sabater, J., Isaksen, L., 2012. Initialisation of land surface variables for numerical weather prediction. Surv. Geophys. http://dx.doi.org/10.1007/s10712-012-9207-x.

de Rosnay, P., Drusch, M., Vasiljevic, D., Balsamo, G., Albergel, C., Isaksen, L., 2013. A simplified extended Kalman filter for the global operational soil moisture analysis at ECMWF. Q. J. R. Meteorol. Soc. 139 (674), 1199–1213.

Dirmayer, P., 2000. Using a global soil wetness dataset to improve seasonal climate simulation. J. Clim. 13, 2900–2921.

Douville, H., Viterbo, P., Mahfouf, J., Beljaars, A., 2000. Evaluation of optimal interpolation and nudging techniques for soil moisture analysis using FIFE data. Am. Meteorol. Soc. 128, 1733–1756.

Drusch, M., Viterbo, P., 2007. Assimilation of screen-level variables in ECMWF's integrated forecast system: a study on the impact of the forecast quality and analyzed soil moisture. Am. Meteorol. Soc. 135, 300–314.

Drusch, M., de Rosnay, P., Balsamo, G., Andersson, E., Bougeault, P., Viterbo, P., 2009a. Towards a Kalman filter based soil moisture analysis system for the operational ECMWF integrated forecast system. Geophys. Res. Lett. 36. http://dx.doi.org/10.1029/2009GL037716.

Drusch, M., Holmes, T., de Rosnay, P., Balsamo, G., 2009b. Comparing ERA-40 based L-band brightness temperatures with Skylab observations: a calibration/validation study using the community microwave emission model. J. Hydrometeorol. 10, 213–226.

Eagleman, J.R., Lin, W.C., 1976. Remote sensing of soil moisture by a 21 cm passive radiometer. J. Geophys. Res. 81, 3660–3666.

Entekhabi, D., Njoku, E.G., O'Neill, P.E., Kellogg, K.H., Crow, W.T., Edelstein, W.N., Entin, J.K., Goodman, S.D., Jackson, T.J., Johnson, J., Kimball, J., Piepmeier, J.R., Koster, R.D., Martin, N., McDonald, K.C., Moghaddam, M., Moran, S., Reichle, R., Shi, J.C., Spencer, M.W., Thurman, S.W., Tsang, L., Van Zyl, J., 2010. The soil moisture active passive (SMAP) mission. Proc. IEEE 98, 704–716.

Fascetti, F., Pierdicca, N., Pulvirenti, L., Crapolicchio, R., Muñoz-Sabater, J., 2016. A comparison of ASCAT and SMOS soil moisture retrievals over Europe and Northern Africa from 2010 to 2013. Int. J. Appl. Earth Observ. 45 (Part B), 135–142.

Figa-Saldana, J., Wilson, J.J.W., Attema, E., Gelsthorpe, R., Drinkwater, M.R., Stoffelen, M.R.A., 2002. The advanced scatterometer (ASCAT) on the meteorological operational (MetOp) platform: a follow on for European wind scatterometers. Can. J. Remote Sens. 28, 404–412.

Hagolle, O., Dedieu, G., Mougenot, B., Debaecker, V., Duchemin, B., Meygret, A., 2008. Correction of aerosol effects on multi-temporal images acquired with constant viewing angles: application to Formosat-2 images. Remote Sens. Environ. 112 (4), 1689–1701.

Hagolle, O., Huc, M., Pascual, D.V., Dedieu, G., 2010. A multi-temporal method for cloud detection, applied to FORMOSAT-2, VENμS, LANDSAT and SENTINEL-2 images. Remote Sens. Environ. 114 (8), 1747–1755.

Houser, P.R., Shuttleworth, W.J., Famiglietti, J.S., Gupta, H.V., Syed, K.H., Goodrich, D.C., 1998. Integration of soil moisture remote sensing and hydrologic modelling using data assimilation. Water Resour. Res. 34, 3405–3420.

Inglada, J., Mercier, G., 2007. A new statistical similarity measure for change detection in multitemporal SAR images and its extension to multiscale change analysis. IEEE Trans. Geosci. Remote Sens. 45 (5), 1432–1445.

Jackson, T.J., Schmugge, T.J., 1991. Vegetation effects on the microwave emission from soils. Remote Sens. Environ. 36, 203–212.

Kerr, Y.H., Waldteufel, P., Wigneron, J.-P., Delwart, S., Cabot, F., Boutin, J., Escorihuela, M., Font, J., Reul, N., Gruhier, C., Juglea, S.E., Drinkwater, M.R., Hahne, A., Martin-Neira, M., Mecklenburg, S., 2010. The SMOS mission: new tool for monitoring key elements of the global water cycle. Proc. IEEE 98 (5), 666–687.

Kerr, Y.H., Waldteufel, P., Richaume, P., Wigneron, J.P., Ferrazzoli, P., Mahmoodi, A., Al Bitar, A., Cabot, F., Gruhier, C., Juglea, S.E., Leroux, D., Mialon, A., Delwart, S., 2012. The SMOS soil moisture retrieval algorithm. IEEE Trans. Geosci. Remote Sens. 50 (5), 1384–1403.

Kerr, Y., Jacquette, E., Al Bitar, A., Cabot, F., Mialon, A., Richaume, P., Quesney, A., Berthon, L., Wigneron, J.-P., 2013. CATDS SMOS L3 Soil Moisture Retrieval Processor: Algorithm Theoretical Baseline Document (ATBD). CESBIO, Toulouse.

Koster, R., Yamada, T.J., Balsamo, G., Berg, A., Boisserie, M., Dirmeyer, P., Doblas-Reyes, F., Drewitt, G., Gordon, C., Guo, Z., et al., 2011. The second phase of the global land-atmosphere coupling experiment: soil moisture contribution to subseasonal forecast skill. J. Hydrometeorol. 12, 805–822.

Massari, C., Brocca, L., Barbetta, S., Papathanasiou, C., Mimikou, M., Moramarco, T., 2014a. Using globally available soil moisture indicators for flood modelling in Mediterranean catchments. Hydrol. Earth Syst. Sci. 18, 839–853.

Massari, C., Brocca, L., Moramarco, T., Tramblay, Y., Didon Lescot, J.-F., 2014b. Potential of soil moisture observations in flood modelling: estimating initial conditions and correcting rainfall. Adv. Water Resour. 74, 44–53.

Massari, C., Brocca, L., Ciabatta, L., Moramarco, T., Gabellani, S., Albergel, C., de Rosnay, P., Puca, S., Wagner, W., 2015. The use of H-SAF soil moisture products for operational hydrology: flood modelling over Italy. Hydrology 2 (1), 2–22.

Merlin, O., Al Bitar, A., Walker, J., Kerr, Y., 2010. An improved algorithm for disaggregating microwave-derived soil moisture based 880 on red, near-infrared and thermal-infrared data. Remote Sens. Environ. 114, 2305–2316.

Mialon, A., Richaume, P., Leroux, D., Bircher, S., Al Bitar, A., Pellarin, T., … Kerr, Y.H., 2015. Comparison of Dobson and Mironov dielectric models in the SMOS soil moisture retrieval algorithm. IEEE Trans. Geosci. Remote Sens. 53 (6), 3084–3094.

Miernecki, M., Wigneron, J.P., Lopez-Baeza, E., Kerr, Y., De Jeu, R., De Lannoy, G.J., … Richaume, P., 2014. Comparison of SMOS and SMAP soil moisture retrieval approaches using tower-based radiometer data over a vineyard field. Remote Sens. Environ. 154, 89–101.

Muñoz Sabater, J., Fouilloux, A., de Rosnay, P., 2012. Technical implementation of SMOS data in the ECMWF integrated forecasting system. IEEE Geosc. Remote Sens. Lett. 9 (2), 252–256. http://dx.doi.org/10.1109/LGRS.2011.2164777.

Muñoz-Sabater, J., 2015. Incorporation of microwave passive brightness temperatures in the ECMWF soil moisture analysis. Remote Sens. 7 (5), 5758–5784. http://dx.doi.org/10.3390/rs70505758.

Muñoz-Sabater, J.M., Jarlan, L., Calvet, J.-C., Bouyssel, F., de Rosnay, P., 2007. From near-surface to root-zone soil moisture using different assimilation techniques. J. Hydrometeorol. 8, 194–206.

Muñoz-Sabater, J., Rudiger, C., Calvet, J.C., Fritz, N., Jarlan, L., Kerr, Y., 2008. Joint assimilation of surface soil moisture and LAI observations into a land surface model. Agric. For. Meteor. 148, 1362–1373. http://dx.doi.org/10.1016/j.agrformet.2008.04.003.

Muñoz-Sabater, J., de Rosnay, P., Balsamo, G., 2011. Sensitivity of L-band NWP forward modelling to soil roughness. Int. J. Remote Sens. 32, 5607–5620.

Naeimi, V., Scipal, K., Bartalis, Z., Hasenauer, S., Wagner, W., 2009. An improved soil moisture retrieval algorithm for ERS and METOP scatterometer observations. IEEE Trans. Geosci. Remote Sens. 47 (7), 1999–2013.

Ni-Meister, W., Walker, J., Houser, P., 2005. Soil moisture initialization for climate prediction: characterization of model and observation errors. J. Geophys. Res. 110. http://dx.doi.org/10.1029/2004JD005745.

Njoku, E.G., Jackson, T.J., Lakshmi, V., Chan, T.K., Nghiem, S.V., 2003. Soil moisture retrieval from AMSR-E. IEEE Trans. Geosci. Remote Sens. 41 (2), 215–229.

Njoku, E.G., Ashcroft, P., Chan, T.K., Li, L., 2005. Global survey and statistics of radio-frequency interference in AMSR-E land observations. IEEE Trans. Geosci. Remote Sens. 43 (5), 938–947.

Oliva, R., Daganzo, E., Kerr, Y.H., Mecklenburg, S., Nieto, S., Richaume, P., Gruhier, C., 2012. SMOS radio frequency interference scenario: status and actions taken to improve the RFI environment in the 1400–1427-MHz passive band. IEEE Trans. Geosci. Remote Sens. 50 (5), 1427–1439.

Owe, M., De Jeu, R.A.M., Holmes, T.R.H., 2008. Multi-sensor historical climatology of satellite-derived global land surface moisture. J. Geophys. Res. 113, F01002. http://dx.doi.org/10.29/2007JF000769.

Pellarin, T., Louvet, S., Gruhier, C., Quantin, G., Legout, C., 2013. A simple and effective method for correcting soil moisture and precipitation estimates using AMSR-E measurements. Remote Sens. Environ. 136, 28–36.

Piles, M., Camps, A., Vall-llossera, M., Corbella, I., Panciera, R., Rudiger, C., Kerr, Y.H., Walker, J., 2011. Downscaling SMOS-derived soil moisture using MODIS visible/infrared data. IEEE Trans. Geosci. Remote Sens. 49 (9), 3156–3166.

Ponziani, F., Pandolfo, C., Stelluti, M., Berni, N., Brocca, L., Moramarco, T., 2012. Assessment of rainfall thresholds and soil moisture modeling for operational hydrogeological risk prevention in the Umbria region (central Italy). Landslides 9 (2), 229–237.

Qiu, J., Crow, W.T., Nearing, G.S., Mo, X., Liu, S., 2014. The impact of vertical measurement depth on the information content of soil moisture times series data. Geophys. Res. Lett. 41 (14), 4997–5004.

Rahmoune, R., Ferrazzoli, P., Singh, Y.K., Kerr, Y.H., Richaume, P., Al Bitar, A., 2014. SMOS retrieval results over forests: comparisons with independent measurements. IEEE J. Select. Top. Appl. Earth Observ. Remote Sens. 7 (9), 3858–3866.

Reichle, R., Koster, R., 2004. Bias reduction in short records of satellite soil moisture. Geophys. Res. Lett. 31. http://dx.doi.org/10.1029/2004GL020938.

Richaume, P., Soldo, Y., Anterrieu, E., Khazaal, A., Bircher, S., Mialon, A., Al Bitar, A., Rodriguez-Fernandez, N., Cabot, F., Kerr, Y., Mahmoodi, A., 2014. RFI in SMOS measurements: update on detection, localization, mitigation techniques and preliminary quantified impacts on soil moisture products. In: EEE International Geoscience and Remote Sensing Symposium (IGARSS), July 13–18, 2014. pp. 223–226.

Scipal, K., Drusch, M., Wagner, W., 2008. Assimilation of an ERS scatterometer-derived soil moisture index in the ECMWF numerical weather prediction system. Adv. Water Resour. 31, 1101–1112.

Soldo, Y., Cabot, F., Khazaal, A., Miernecki, M., Slominska, E., Fieuzal, R., Kerr, Y.H., 2015. Localization of RFI sources for the SMOS mission: a means for assessing SMOS pointing performances. IEEE J. Select. Top. Appl. Earth Observ. Remote Sens. 8 (2), 617–627.

Stoffelen, A., 1998. Toward the true near-surface wind speed: error modeling and calibration using triple collocation. J. Geophys. Res. 103 (C4), 7755–7766.

Tomer, S.K., Al Bitar, A., Sekhar, M., Zribi, M., Bandyopadhyay, S., Sreelash, K., Sharma, A., Corgne, S., Kerr, Y., 2015. Retrieval and multi-scale validation of soil moisture from multi-temporal SAR data in a semi-arid tropical region. Remote Sens. 7 (6), 8128–8153.

Verhoest, N.E.C., van den Berg, M.J., Martens, B., Lievens, H., Wood, E.F., Pan, M., Kerr, Y.H., Al Bitar, A., Tomer, S.K., Drusch, M., Vernieuwe, H., De Baets, B., Walker, J.P., Dumedah, G., Pauwels, V.R.N., 2015. Copula-based downscaling of coarse-scale soil moisture observations with implicit bias correction. IEEE Trans. Geosci. Remote Sens. 53 (6), 3507–3521. http://dx.doi.org/10.1109/TGRS.2014.2378913.

Wagner, W., Lemoine, G., Rott, H., 1999. A method for estimating soil moisture from ERS scatterometer and soil data. Remote Sens. Environ. 70, 191–207.

Wagner, W., Hahn, S., Kidd, R., Melzer, T., Bartalis, Z., Hasenauer, S., Figa, J., de Rosnay, P., Jann, A., Schneider, S., Komma, J., Kubu, G., Brugger, K., Aubrecht, C., Zuger, J., Gangkofner, U., Kienberger, S., Brocca, L., Wang, Y., Bloeschl, G., Eitzinger, J., Steinnocher, K., Zeil, P., Rubel, F., 2013. The ASCAT soil moisture product: a review of its specifications, validation results, and emerging applications. Meteorol. Z. 22 (1), 5–33.

Walker, J.P., Willgoose, G.R., Kalma, J.D., 2001. Onedimensional soil moisture profile retrieval by assimilation of near-surface measurements: a simplified soil moisture model and field application. J. Hydrometeorol. 2, 356–373.

Wanders, N., Pan, M., Wood, E.F., 2015. Correction of real-time satellite precipitation with multi-sensor satellite observations of land surface variables. Remote Sens. Environ. 160, 206–221.

Wang, J.R., Choudhury, B.J., 1981. Remote sensing of soil moisture content over bare field at 1.4 GHz frequency. J. Geophys. Res. 86, 5277–5282.

Wigneron, J.P., Kerr, Y., Waldteufel, P., Saleh, K., Escorihuela, M.J., Richaume, P., Ferrazzoli, P., de Rosnay, P., Gurney, R., Calvet, J.C., Grant, J.P., Guglielmetti, M., Hornbuckle, B., Mätzler, C., Pellarin, T., Schwank, M., 2007. L-band microwave emission of the biosphere (L-MEB) model: description and calibration against experimental data sets over crop fields. Remote Sens. Environ. 107 (4), 639–655. Au12

Wood, E.F., Roundy, J.K., Troy, T.J., van Beek, L.P.H., Bierkens, M.F.P., Blyth, E., de Roo, A., Döll, P., Ek, M., Famiglietti, J., Gochis, D., van de Giesen, N., Houser, P., Jaffë, P.R., Kollet, S., Lehner, B., Lettenmaier, D.P., Peters-Lidard, C., Sivapalan, M., Sheffield, J., Wade, A., Whitehead, P., 2011. Hyperresolution global land surface modeling: meeting a grand challenge for monitoring earth's terrestrial water. Water Resour. Res. 47, W05301.

# Non-Print Items

**Abstract:**

This chapter provides a description of current operational applications using state-of-the-art soil moisture retrievals from active and passive remote sensing data. Both types of observations have demonstrated to contain useful information of shallow land variables. In particular, this chapter focuses on how soil moisture retrievals are used at the operational level to derive flood, drought, and landslides warnings, as well as its use in coupled land-atmospheric models. An overview of the caveats in the production and applications of the retrievals is also provided. The chapter ends by providing perspectives of these novel applications.

**Keywords:** soil moisture; microwave active data; microwave passive data; retrievals; operational.